

LiM 2011

Simulation and Technology of Hybrid Welding of Thick Steel Parts with High Power Fiber Laser

Gleb Turichin^{a,*}, Ekaterina Valdaytseva^a, Igor Tzibulsky^a,

Alexander Lopota^b, Olga Velichko^b

^a*Institute of Laser and Welding Technology, SPbSPU, St. Petersburg 195251, Russia*

^b*LTC Ltd, St. Petersburg 194064, Russia*

Abstract

The article devoted to steady state and dynamic simulation of melt pool behavior during hybrid laser-arc welding of pipes and shipbuilding sections. The quasi-stationary process-model was used to determine an appropriate welding mode. The dynamical model of laser welding was used for investigation of keyhole depth and width oscillations. The experiments of pipe steel and stainless steel hybrid laser-MAG welding have been made with 15-kW fiber laser in wide range of welding mode parameters. Comparison of experimentally measured and simulated behavior of penetration depth as well as their oscillation spectra approved the self-oscillation nature of melt pool behavior. The welding mode influence of melt pool stability has also been observed. The technological peculiarities, which allow provide high quality weld seam, has been discussed also.

Keywords: laser welding, hybrid welding, simulation

1. Introduction

Idea to use together laser radiation and electric arc for welding of metals so that both of heat sources influence on a product within the limits of one heating zone, was born more then 30 years ago [1]. Until recently powerful CO₂-lasers were applied, they generated radiation with wavelength of 10.6 microns. Interaction of radiation of this wavelength with metals is accompanied by beginning of the optical discharge in the influence zone that effect essentially on the focused beam parameters and part of the absorbed energy in the target and plasma in the interaction zone. Interaction of laser radiation of wavelength 1.06 microns with the target is essentially different. However, powerful lasers with such wavelength had poor radiation quality and small reliability. Only recently technological ytterbium fiber lasers with continuous radiation power range up to 30 kW were developed, they possess high beam quality and high reliability.

Hybrid laser arc welding is one of the most prospective technologies for joining of thick and heavy parts for shipbuilding, production of gas and oil pipes, bridge sections and building constructions. The main advantage of

* Corresponding author. Tel.: +7-812-552-95-79; Fax: +7-812-552-98-43.
E-mail address: gleb@ltc.ru.

hybrid welding is a possibility to weld by one path materials with thickness up to 15 mm and more, including new high strength steels and modern alloys. In spite of hybrid welding can provide high quality weld seam which properties are comparable with laser welding weld seam properties, the usage of this technology in the case of real production is restricted by high complicity of the process [2] and appearance of porosity, cracks, spiking and humping in the weld seam, especially in welding of alloyed steels.

The analysis of results of the fulfilled researches of laser arc welding process enables to define a number of problems which decision is necessary to develop reliable technology of welding of thick metals. In particular, it is necessary to eliminate: sharp increase of the seam width in the top part of its cross section; an unwanted direction of crystals growth; presence of hardening structures in deep penetration zone; presence of set of gas pores; unsatisfactory values of impact strength of the axial zone, especially at negative test temperatures. The overview of modern trends and problem for solution is presented in [3]. Due to high complicity of the process the only way to develop a reliable technology of hybrid welding is use a model based simulation for the determination and optimizing of technological parameters as well as for finding and testing of technological methods.

2. Simulation of the process of hybrid laser-arc welding

For simulation of weld bath formation and behavior during hybrid laser-arc welding two process models, one for steady state modeling, and second for modeling of melt pool dynamic behavior, have been developed. The steady state model based on the model of laser welding with deep penetration, described in [4]. Model include a solution of the number of connected tasks, such as: laser beam interaction with laser induced and arc plasma with consideration of gas dynamics of plasma and shielding gas jet, kinetics of hybrid laser-arc discharge in metal vapor-shielding gas mixture above the workpiece surface, arc current flow, filler wire heating and melting, laser beam absorption and multiply reflection in the keyhole, heat-mass transfer in melt and solid face, evaporation and vapor flow dynamics in the keyhole. All partial models take into account the main peculiarities of related physical processes. Task about laser beam absorption and reflection inside the keyhole, heat transfer task in solid face and task about vapor flow in keyhole are solved by the same way as it was done for the model of laser welding [4]. The arc and plasma models use boundary layer approximation for mass, momentum, current and energy equations [5]. Media compressibility, volumetric heating by laser beam and arc current, mixing of metal vapor, shielding and arc gas, temperature influence on kinetic coefficients are taken into account as well as workpiece surface influence on arc and shielding gas flow. The discharge model, which determine a values of ionization rate, and, therefore, spatial distributions of conductivity and thermal diffusivity, based in solution of Raizer kinetic equation with consideration of electron exchange between plasma and metal condensate in the plasma plume. The filler wire melting task solved in one-dimension approach with consideration of Stephan conditions on solid-liquid interface and electric force action on drops transfer [6]. For solution of melt flow and heat transfer task in the liquid phase the approximation of potential flow of ideal liquid with viscous boundary layers on the melting front and keyhole surface has been used. To take into account influence of gap between welding parts the hydrodynamic task has been solved as 3D task differently with the model for laser welding.

The scheme of process model is shown on Figure1 Different tasks are connected as through boundary conditions; when solution of one task determine boundary condition for another, as through direct influence of equation coefficients.

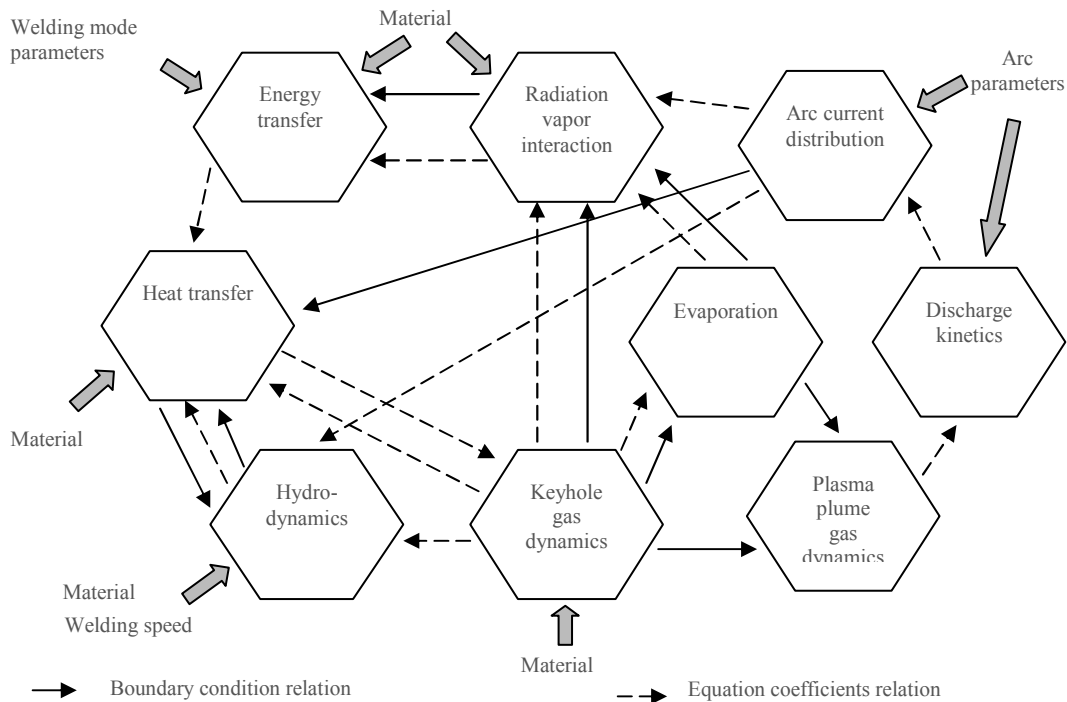


Figure 1. Structure of steady state process model.

For mathematical solution of this complex problem the specially developed numerical-analytical algorithm, similar to described in [7], has been used. The algorithm has been implemented to the LaserCAD system, that allows simulate a shape and size of melt pool as well as temperature distribution in weld bath and HAZ during hybrid laser-MAG welding.

Second model which is necessary for the technology development is a model of melt pool dynamic behavior. It was developed on the base of dynamic model of laser welding process [8]. The model based on the formalism of Lagrange mechanics, that allow take into account such phenomena as: wave movement of the cavity surface, change of the shape and sizes of the weld bath in time and influence of the cavity motion as the whole on oscillations of its depth and radius. The friction forces effect has been also added into the movement equation. We'll consider geometry of the model and its possible simplifications before deriving equations of motion by Lagrange formalism. Such simplifications as $H \gg a$, where "H" is a penetration depth and "a" is a keyhole radius, and neglecting by inclination of the cavity and melt bath walls was assumed. The melt flow was assumed as potential flow that answer Laplace's equation.

$$s(z) = s_0 + \sum_{n=1}^{\infty} s_n \cos \frac{\pi n z}{H}$$

for the area of vapor cavity cross section $s(z)$ in the motionless (in respect to the target) coordinate system, one can get expression for the velocity v_z along the keyhole axe:

$$V_z = \frac{1}{S-s} \left(\dot{s}_0 z + s_0 \dot{H} + \sum_{n=1}^{\infty} \frac{\dot{s}_n H}{\pi n} \sin \frac{\pi n z}{H} \right)$$

where "S" is area of melting front cross section.

As melt flow consist of the flow along the keyhole axe "z" v_z and flow in the cross section plane v_{\perp} , the kinetic energy of the melt pool consist of three parts: $E = E_{\perp} + E_z + E_b$, where, as it possible to calculate:

$$E_{\perp} = \pi H a^2 \left(\frac{\rho V_0^2}{2} \frac{A^2 + a^2}{A^2 - a^2} + \frac{\rho a^2}{2} \frac{A^4}{(A^2 - a^2)^2} \left\{ \ln \frac{A^2}{a^2} - 2 \left(1 - \frac{1}{2} \frac{a^2}{A^2} \right)^2 + \frac{1}{2} \right\} \right)$$

$$E_z = \frac{\rho}{2(S - s_0)} \left\{ s_0^2 H^2 \left(\frac{1}{3} + \sum_{n=1}^{\infty} (-1)^n \frac{2s_n}{(\pi n)^2 (S - s_0)} \right) + s_0^2 \dot{H}^2 H + \sum_{n=1}^{\infty} \frac{H^3 \dot{s}_n^2}{2(\pi n)^2} + \right.$$

$$+ s_0 H^2 \dot{s}_0 \dot{H} \left(1 + \sum_{n=1}^{\infty} \frac{2((-1)^n - 1)s_n}{(\pi n)^2 (S - s_0)} \right) + \sum_{n=1}^{\infty} \sum_{k=1}^{\infty} \frac{1}{2} \dot{s}_0 \dot{s}_n (s_{n-k} - s_{n+k}) \frac{H^3}{p^2 n k (S - s_0)} -$$

$$- \sum_{n=1}^{\infty} (-1)^n \dot{s}_0 \dot{s}_n \frac{H^3}{\pi^2 n} \left[\frac{2}{n} + \sum_{k=1}^{\infty} (-1)^k \frac{1}{\pi} \frac{s_k}{S - s_0} \left(\frac{1}{(n+k)^2} + \frac{1 - \delta_{nk}}{(n-k)^2} \right) \right] +$$

$$\left. + \sum_{n=1}^{\infty} s_0 H^2 \dot{s}_n \dot{H} \frac{1}{\pi^2 n} \left[\frac{2(1 - (-1)^n)}{n} - \sum_{k=1}^{\infty} \frac{s_k}{S - s_0} \left(\frac{(-1)^{n+k} - 1}{n+k} + \frac{1 - \delta_{nk}}{n-k} \right) \right] \right\}$$

where “A” and “a” are radii of the images of melting front and keyhole cross sections after their conform mapping on concentric circle.

E_b is energy of motion in the melt pool bottom part:

$$E_b = \frac{\rho}{2} \frac{4\pi a^2 A^2}{(A^2 - a^2)^2} \dot{H}^2 \sum_{i=1}^{\infty} \frac{J_1(\sqrt{\lambda_i} a) \frac{1}{4} \left(e^{4\sqrt{\lambda_i}(L-H)} - 1 \right) e^{-2\sqrt{\lambda_i}(L-H)}}{\lambda_i^{3/2} s h^2 (\sqrt{\lambda_i}(L-H)) J_0(\sqrt{\lambda_i} A)},$$

where λ_i is a root of the equation $J_1(\lambda_i) = 0$.

Since potential energy of the active zone is superficial energy, it is enough to calculate a free surface area and multiply it by the value of the specific surface energy been equal to surface tension coefficient “σ”:

$$\Pi = \sigma \left\{ \pi A^2 + 2\pi a H + \frac{\sqrt{\pi}}{4} \sum_{n=1}^{\infty} \frac{n^2 s_n^2}{H \sqrt{s_0}} + 2H_1(A + a) \right\},$$

Where H_1 is elevation of melt surface on workpiece surface.

The expressions for generalised forces Q_i that corresponds to chosen generalised coordinates (s_0, s_n, H) have been obtained by using definition:

$$Q_i = \frac{\delta A_i}{\delta q_i},$$

where δA_i is a virtual work on the virtual displacement δq_i . For Q_H it is easy to get:

$$Q_H = (p - p_0) s_0,$$

where “p” is a vapour pressure inside the cavity, p_0 is an external pressure. Taking into account the vapour jet reactive force finally one can get:

$$Q_H = \left(p - p_0 + \rho_0 v_0^2 \right) \cdot s_0 ,$$

where ρ_0 and v_0 - correspondingly density and velocity of recoil vapour jet in the workpiece surface plane. For Q_s after several transformations, it is possible to obtain:

$$Q_{s_0} = \left(p(s_0) - p_0 \right) H - \frac{1}{3} \frac{\sigma}{a} H + (-1)^n \frac{2}{\pi^2} \frac{\sigma s_n}{a s_0} \frac{H}{n^2}$$

$$Q_{s_n} = H \left[\frac{\partial p}{\partial s} \Big|_{s=s_0} \frac{s_n}{s_0} + \frac{\sigma s_n}{a s_0} (-1)^n \frac{1}{\pi^2 n^2} + \frac{2}{\pi^2} \frac{\sigma}{a} \sum_{\substack{k=1 \\ k \neq n}}^{\infty} \frac{s_k}{s_0} (-1)^{n+k} \frac{n^2 + k^2}{(n^2 - k^2)^2} \right]$$

To determine $p(s_0)$ and $\frac{\partial p}{\partial s} \Big|_{s=s_0}$ the non-stationary heat transfer problem has been solved analytically.

To introduce generalized viscous forces according to Lagrange mechanics formalism, the dissipative function

$$D = \frac{dE}{dt}$$

has been derived, and the generalised friction force

$$R_i = \frac{1}{2} \frac{\partial D}{\partial Q_i}$$

has been calculated. Solving task about the melt flow in the boundary layer at the melting front gives following expression for the dissipative function:

$$D_1 = -\rho L \sqrt{\frac{v}{\pi}} \int_{-\infty}^t \frac{d\tau}{\sqrt{t-\tau}} \cdot \int_0^H \frac{dV_0}{d\tau} V_0(t) dz$$

where L - melting front perimeter ($L = 2\pi A$).

Having derived kinetic and potential energy of the object as well as generalized forces, one can get a system of Lagrange equations (dynamic model one) imagined as:

$$\frac{d}{dt} \frac{\partial L}{\partial \dot{q}_i} - \frac{\partial L}{\partial q_i} = Q_i + R_i ,$$

where q_i assumes $H, s_0, s_1, \dots, s_n, \dots$ consecutively.

To fulfill calculates the system was “cut” in s_2 and the system obtained from four ordinary differential equations of second order was solved numerically by standard 6-th order Runge-Kutt algorithm. The test calculations was made for laser welding of mild steel in the power scale from 1 up to 20 kW and welding velocity from 0.3 till 10 cm/sec. This algorithm was also implemented to the LaserCAD.

The developed mathematical formalism allows using it for the dynamic analysis of occurrence of porosity and spiking, as it shown on Figure 2 for example.

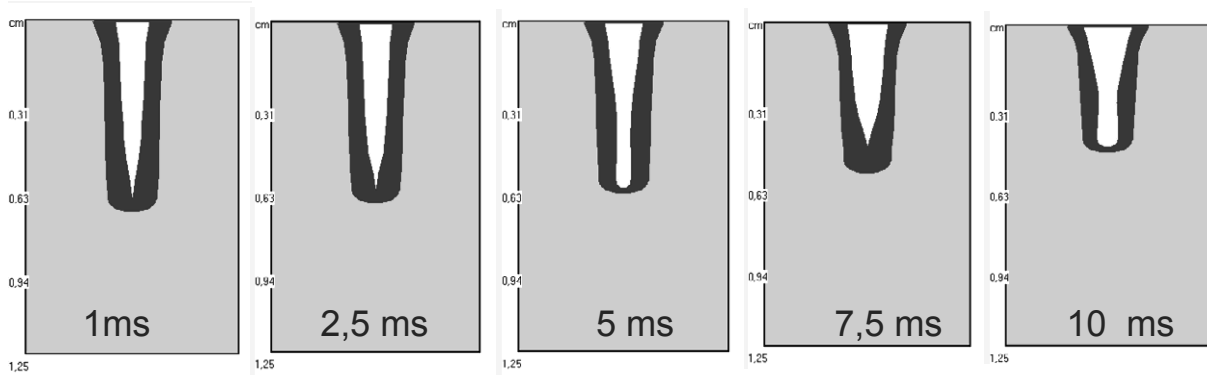


Figure 2. Simulation of dynamic behavior of the welding bath at hybrid laser-arc welding, material – Steel 10, laser radiation power is 4.5 kW, welding speed is 12 mm/s, beam focal radius is 0.2 mm, focal distance is 30 cm, electric arc power is 2.5 kW.

Analysis of the calculations results shows that, dense occupation of the limited regions on the phase portraits by the phase trajectories says about turbulent character of the cavity oscillations. It explains the calculation results independence from initial conditions (when the initial point gets into the attractor). Sizes and shape of the attractor are determined by welding regime parameters.

Modelling show, that as it was for the laser welding, for the hybrid welding different generalized co-ordinates have the different oscillations spectra. The lowest frequencies (less than 100 Hz) are typical for cavity radius and depth oscillations. Increases of penetration depth and filler material rate lead to spectrum shift in low frequency direction. The first (s_1) and second (s_2) order waves have the highest frequency spectra (up to 10 kHz). These spectra are also depend on the cavity depth. The feeding velocity increasing also decreases the low-frequency oscillations.

Developed model can be used for dynamical analysis of porosity appearance and spiking phenomena (Figure 3).

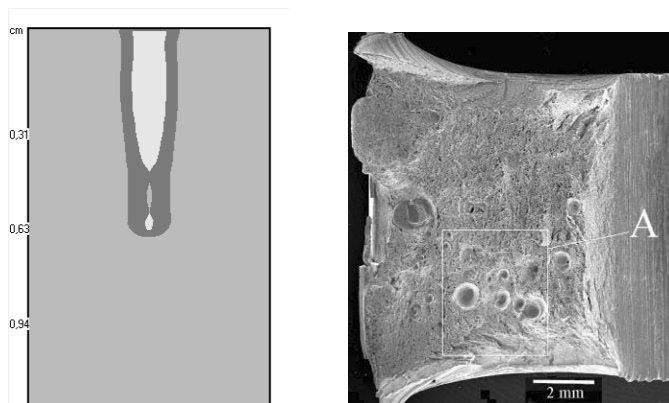


Figure 3. Simulation of porosity appearance due to cavity collapse (left) and results of experiment

3. Technological installation design for hybrid laser-arc welding

The technological installation which has been developed for hybrid laser-MAG welding of thick steel parts has provide welding of steel sheets of thickness more then 12 mm together with an arc source by one pass with a speed up to 3 m/min. Simulation with LaserCAD allowed determine parameters of installation: laser source power is not

less than 15 kW; beam diameter in focus is 0.3-0.4 mm; welding current is not less than 250 A, diameter of the electrode wire is in range of 1 ... 2 mm.

The developed complex consists of: Fiber laser LS-15 manufactured by IPG with chiller Riedel PC250, arc power source VDU-1500 with current up to 1500 A and numerical control filler wire feeding equipment, laser-arc module (the working tool), 6 channels CNC module of preparation and distribution of gases, system of monitoring of the welded joint and tracking on the base of scanner laser sensor, system of process monitoring and control system.

The laser-arc module is intended for work in technological complexes for hybrid laser-arc welding of high thickness metals. It consists of: manipulator, laser welding head, arc welding torch, sensor of the seam tracking system, sensor of the process monitoring system. Gas protection of the weld is also provided. Developed equipment is shown on Figure 4.

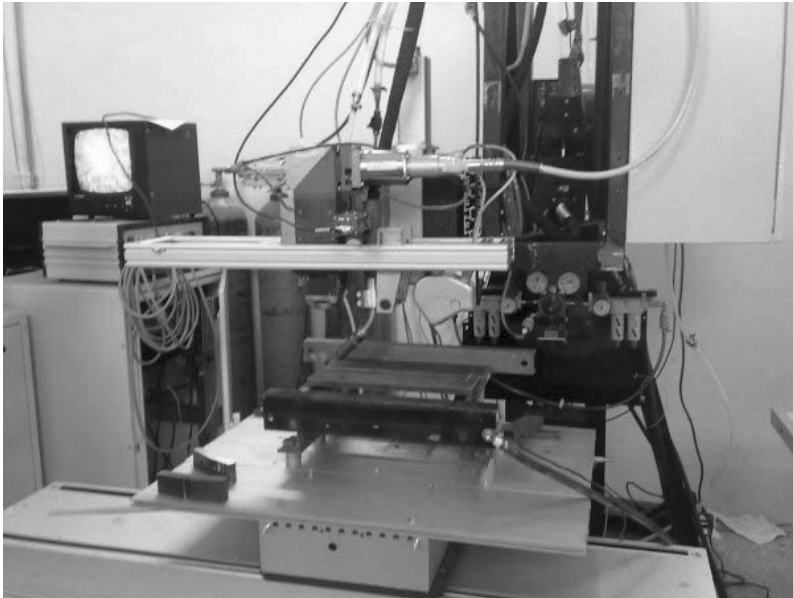


Figure 4. Hybrid laser-MAG welding installation

Control and stabilization of position of the hybrid laser-arc module relative to the joint is fulfilled by drives system. It operates the executing devices of the manipulator, such as keep of position of the focus point of the laser head relative to welded surfaces (“vertical moving”), keep of positions of the focus point of the laser head relative to the joint (“cross moving”).

Accuracy of keep of the focus point position of the laser head in relative to welded surfaces in the vertical direction is ± 0.2 mm. Accuracy of keep of the focus point position of the laser head in relative to the joint in the cross-section direction is ± 0.5 mm

The laser welding head of “Precitec YW 50” incorporates a scanning device to mix the melt in the welding bath.

The control system of the laser-arc complex is realized as a hardware-software complex. This is a distributed computing operating system, which manages all components of the welding complex and consists of the welding joint monitoring subsystem, the welds monitoring subsystem and automatic control system.

The control system carries out: reading of a joint profile of welded sheets, control of the joint geometrical characteristics, tracking coordinates of the joint at welding speed up to 6 m/min, positioning of the welding head above the welded joint; control of the laser radiation source, control of the arc source, control of protective gases feed, control of the welding process parameters and their documenting, measurement of the welding head

parameters and protection against invalid modes, on-line quality control of the welds by using the process-monitoring.

According to solved problems the control system consists of several subsystems: control of the laser; control of the arc equipment; control of the gas equipment; welding head positioning; reading of the metal joint geometry; the control of parameters and protection of the laser welding head; the module of the central controller; an operating computer. To communicate with other modules of the complex a card of CAN interface is placed into the computer.

4. Development of technology on the base of process-simulation

Simulation of process of hybrid laser-arc welding by means of computer program LaserCAD has allowed predicting the weld shape depending on the set parameters of energy sources and material. An example of simulation of hybrid welding of steel AISI 1330 is shown on the figure 5. The steady state model of process, implemented in LaserCAD, include connected physically adequate models of heat-mass transfer in solid, liquid and gas phase, radiation transfer and kinetics of combined laser-arc discharge. There are shown also calculation of cross-section of the melting and heat affected zones, and the calculated thermal cycles combined with continuous cooling transformation diagram, allowing to estimate phase-structure combination of metal.

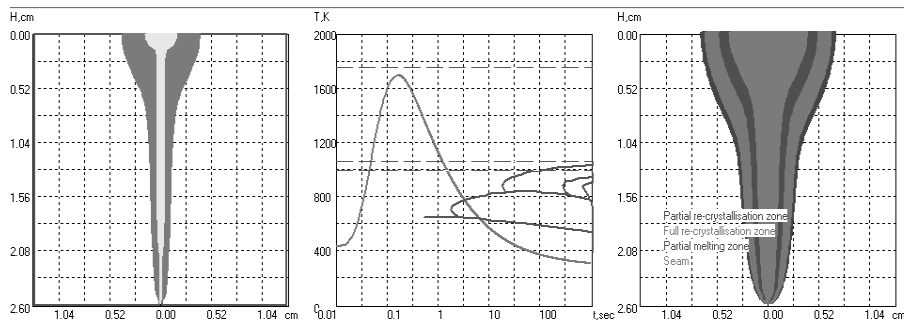


Figure 5. Results of mathematical simulation of laser and hybrid welding of steel AISI 1330 (10 kW + 4 kW).

The given model allows to estimate demanded parameters of heating sources, to predict phase-structure of metal combination after welding and thereby to lower number of experiments. The dynamical models of laser welding process, allows using it for the dynamic analysis of occurrence of porosity and spiking, and find the way of decreases of dynamic instabilities on melt pool behavior, such as beam scanning introduction, as it shown on figures 6, 7 for example.

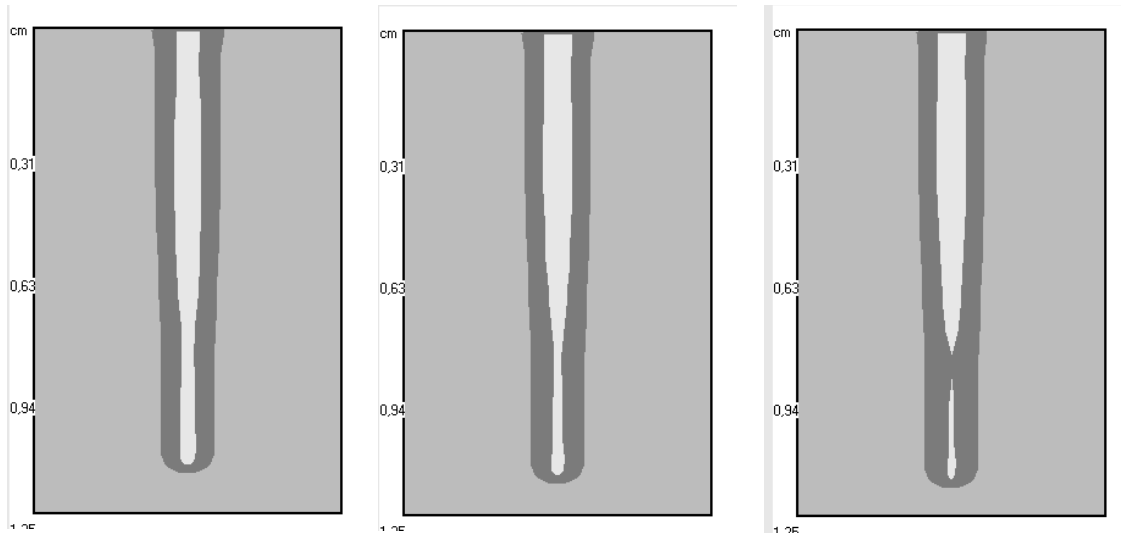


Figure 6. Simulation of dynamic behavior of the welding bath at hybrid laser-arc welding with temporal step 3 ms, material – Steel 10G2FBU, laser radiation power is 14.5 kW, welding speed is 4 cm/s, beam focal radius is 0.2 mm, focal distance is 30 cm, electric arc power is 2.5 kW.

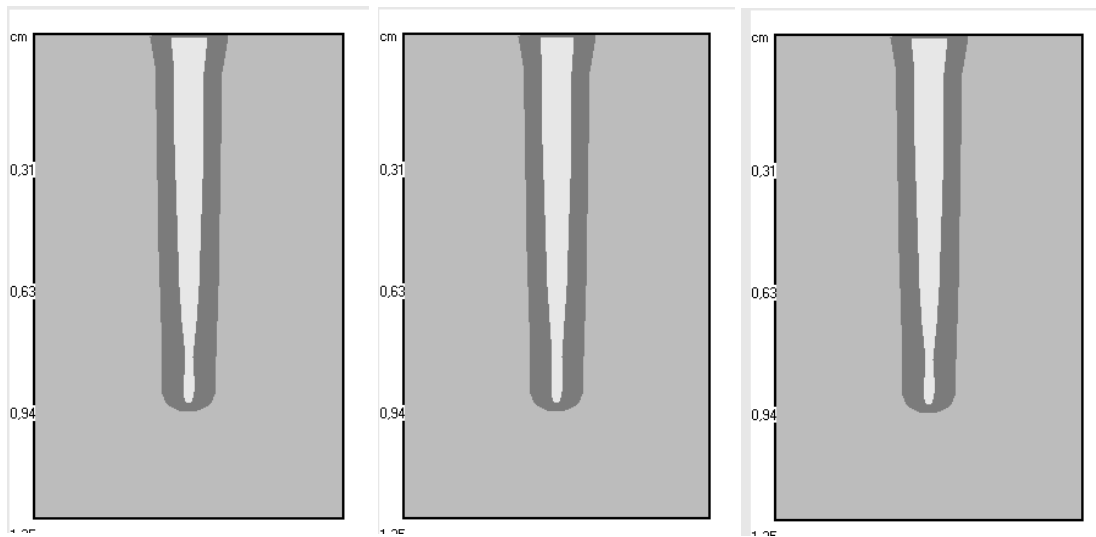


Figure 7. Simulation of dynamic behavior of the welding bath at hybrid laser-arc welding with temporal step 3 ms, material – Steel 10G2FBU, laser radiation power is 14.5 kW, welding speed is 4 cm/s, beam focal radius is 0.2 mm, focal distance is 30 cm, beam scanning frequency 400 Hz, scanning amplitude 0.2 mm, electric arc power is 2.5 kW.

During experiments the plane samples with thickness of 8 mm, 10 mm, 12 mm, 24 mm from steels St3, 25G2S, 10G2FBU, 12Ch18N9T were melted and welded in butt joint. Welding was carried out as rectilinear butt seams in bottom spatial position. Argon, welding dioxide of carbon and their mixes were used to protect welding bath and seam metal. A coaxial protective gas jet nozzle and non-coaxial protection of the welding bath were used additionally. Quality of all welded seams was estimated visually on their appearance, on the base of metallographic researches of cross-sections, with x-rays investigation and with standard mechanical tests. The penetration depth and

other seam geometry parameters were determined as well as defects presence and material properties in weld seam and HAZ. The different technology for different thickness of welding parts has been developed (Figure 8).

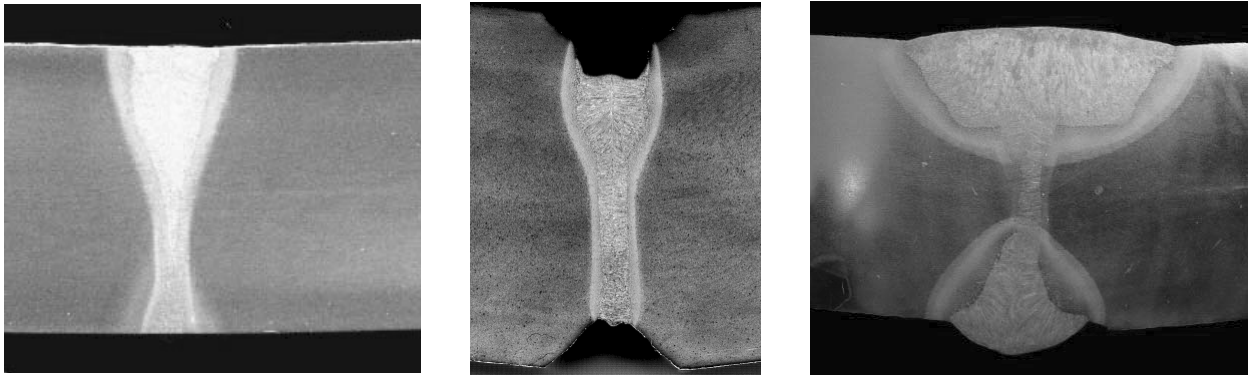


Figure 8 – Macro section of the one pass weld (left), and three passes weld (center – first technological pass, right – technological pass and two filled passes by submerged arc welding. Depth is 15 mm left and 24 mm center and right. Material is pipe steel X 80.

5. Result and discussion

With the help of steady state and dynamic simulation the process design and welding mode parameters, which provide high quality seam even in the case of large value of gap between welded parts up to 2 mm, have been developed. Also usage of beam scanning, optimization of arc torch position relative laser beam, optimization of composition of arc gas mixture together with usage of special filler wire with nanopowder admixtures, which was developed for this process, allow to avoid appearance of such defects, as porosity, hot cracks and humping, and provide value of impact energy on temperature -40 C in the bounds of 140 – 200 J for pipe steel X80.

References

- [1] Patent 1547172 Great Britain, MKI V23K 26/00, 9/00. Methods and apparatus for cutting, welding, drilling and surface treating / W. M. Steen. - Publ. 06.06.79
- [2] F. O. Olsen, Hybrid laser arc welding, SRS Press, 2009, 320 p.
- [3] B. Ribic, T. A. Palmer and T. DebRoy, Problems and issues in laser-arc hybrid welding, International Materials Reviews, 2009, V. 54, N 4, p. 223-244
- [4] Vitaliy A. Lopota; Yuri T. Sukhov; Gleb A. Turichin, Computer simulation of laser beam welding for technological applications, SPIE Proc V. 3091, 1997, p. 19-23
- [5] G. A. Turichin, A. M. Grigor'ev, E. V. Zemlyakov, E. A. Valdaitseva, U. Dilthey and A. Gumenuik: High Temp., 2006, 44, 647–655
- [6] G. Turichin, E. Pozdeeva, E. Zemlyakov, Numerical-analytical model of electrode wire melting in laser-arc welding, Physics and chemistry of material processing, 2007. № 4. p. 41-45./rus/.
- [7] Beyer E., Dahmen M., Fuerst B., Kreutz E. W., Nitsch H., Turichin G., Schulz W. «A Tool for Efficient Laser Processing», Proceedings of 14 Int. Congress on application of lasers - ICALEO-95, San Diego, USA.
- [8] G. Turichin, E. Valdaitseva, E. Pozdeeva, U. Dilthey, A. Gumenuik. Theoretical investigation of dynamic behavior of molten pool in laser and hybrid welding with deep penetration, Paton welding journal, 2008 (7), p. 11-15